Extremely anisotropic suppression of huge enhancement of electrical resistivity by magnetic field in α-R2S3 (R = Sm, Dy).

Journal of Physics: Conference Series

Extremely anisotropic suppression of huge enhancement of electrical resistivity by magnetic field in α-R_2S_3 (R = Sm, Dy)

IOP Conf. Series: Journal of Physics: Conf. Series **969** (2018) 012124 doi:10.1088/1742-6596/969/1/012124

Extremely anisotropic suppression of huge enhancement of electrical resistivity by magnetic field in α-R_2S_3 (R = Sm, Dy)

S Ebisu, T Era, Q Guo and M Miyazaki

Division of Applied Sciences, Muroran Inst. of Tech., 27-1 Mizumoto-cho, Muroran 050-8585, Hokkaido, Japan

ebisu@mmm.muroran-it.ac.jp

Abstract. The electrical resistivity ρ and magnetization M of α-R_2S_3 (R = Sm, Dy) single crystals have been measured in various magnetic fields lying in the *ac*-plane of an orthorhombic crystal structure. The measurements have been carried out by rotating the single crystals around the *b*-axis (being set parallel to a horizontal direction), corresponding to the longitudinal direction of needle-shaped single crystals, in vertical magnetic fields. The electrical resistivity under no magnetic field shows huge enhancement in a narrow temperature range around the successive magnetic transition temperatures, as reported previously. Such enhancement is suppressed rapidly by applying a magnetic field, which has been clearly seen as diminishing of the $\rho(T)$ peak. The magnetic field along the easy magnetization axis; H_{easy}, moves the $\rho(T)$ peak toward higher temperature with diminishing it, while the magnetic field along the hard magnetization axis; H_{hard}, moves it to lower temperature. The suppression effect is extremely anisotropic for the orientation of the magnetic field lying in the *ac*-plane. It has been concluded that H_{easy} suppresses the ρ enhancement most strongly. The suppression effect under H_{easy} is more than 200 times larger at least in some cases than that under H_{hard}.

1. Introduction

Rare earth sesquisulfides α-R_2S_3 (R = Sm and Dy) have attracted much attention because of their novel physical properties brought about by successive magnetic transitions [1-6]. These compounds and other rare earth compounds α-R'_2S_3 (R' = La, Ce, Pr, Nd, Gd and Tb) have the α-Gd_2S_3 type crystal structure with the *Pnma* symmetry shown in figure 1 [7-9]. There are two crystallographically inequivalent R sites labeled with $R1$ and $R2$ in this structure. We have found fascinating physical properties in both series compounds α-R_2S_3 and α-R'_2S_3 (except R' = La, Ce). Briefly speaking only about the magnetic properties in α-R'_2S_3, they are as follows. The α-Gd_2S_3 shows only one antiferromagnetic (AFM) transition at T_N = 9.9 K [10-13], while the α-Tb_2S_3 shows successive AFM transitions at T_{N1} = 12.5 K and T_{N2} = 3.5 K [3, 14, 15]. The α-Nd_2S_3 also shows successive transitions at T_N = 2.75 K and the temperature around 0.65 K suggesting magnetic ordering [16]. The α-Pr_2S_3 shows an AFM transition at T_N = 2.95 K, as well as Van Vleck paramagnetic contribution. The ground term of one Pr site atoms has been considered to be singlet and Pr atoms on the other site seem to demonstrate magnetic ordering partially at T_N. Remaining degrees of freedom have been inferred to disappear by ordering below 1 K from the specific heat data [16].

The physical properties of α-R_2S_3 (R = Sm and Dy) are outstandingly attractive. The α-Dy_2S_3 also exhibits successive AFM transitions at T_{N1} = 11.4 and T_{N2} = 6.4 K [2]. As for α-Sm_2S_3, weak ferromagnetic (WFM) properties were observed around 4 K in the temperature dependence of the magnetic susceptibility [4]. Recent our study on the specific heat of the α-Sm_2S_3 has clarified that successive WFM transitions occur at T_{C1} = 3.8 K and T_{C2} = 1.9 K, which will be reported elsewhere. We have also found extremely broad hysteresis in magnetization process of α-Dy_2S_3 after cooling in the magnetic field of 18 T [5]. Furthermore, easy magnetization axes in the *ac*-plane of both the α-Sm_2S_3 and α-Dy_2S_3 are surprisingly exchangeable between ***a*** and ***c*** after some processes of changing the magnetic field orientation and temperature, which will be reported by S Ebisu *et al*. elsewhere. The most fascinating property of α-R_2S_3 is a huge enhancement and restoration of the electrical resistivity for the single crystals seen in a narrow temperature range of a few Kelvin just above T_{N2} for α-Dy_2S_3 and T_{C1} for α-Sm_2S_3 [1, 4]. The magnitude of the enhancement is more than 10 times for α-Dy_2S_3 and 100 times for α-Sm_2S_3, although the magnitude depends on single crystal sample (i.e. an amount of some lattice imperfections). This phenomenon forms a sharp peak in the temperature dependence of the electrical resistivity $\rho(T)$. Another small peak is also observed just below T_{N2} or T_{C1} in the $\rho(T)$ for each compound. Furthermore, the huge enhancement of the electrical resistivity measured along the *b*-axis corresponding longitudinal direction of the needle-shaped single crystal is suppressed rapidly by applying the magnetic field perpendicular to the *b*-axis. The needle-like shape of these single crystals suggests that these compounds have strong uniaxial anisotropies along the *b*-axis for physical properties. Moreover, considering the crystal structure of the α-R_2S_3, anisotropies in the *ac*-plane do not seem to be negligible. In this paper, we will report anisotropic suppression effect of huge enhancement of the electrical resistivity in the α-Sm_2S_3 and α-Dy_2S_3 single crystals by the magnetic field lying in the *ac*-plane.

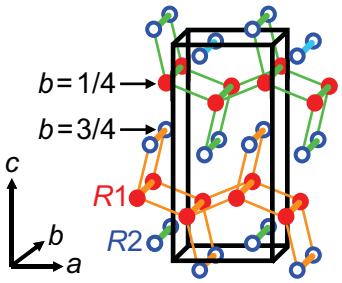

Figure 1. Crystal structure of α-R_2S_3, in which only the R atoms are shown for clarity. The R atoms are located on two crystallographically inequivalent R sites labelled with $R1$ (closed circles) and $R2$ (open circles). Thin lines are drawn between neighbor atoms on the same *ac*-plane (b = 1/4 or 3/4). The orthorhombic unit cell is also shown as a box.

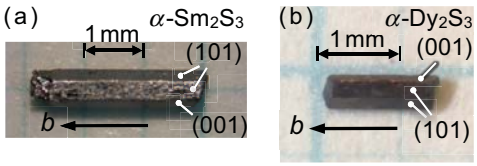

Figure 2. Single crystal of (a) α-Sm_2S_3 and (b) α-Dy_2S_3. The longitudinal direction of the needle-like shape corresponds to the *b*-axis of the orthorhombic crystal system. They have a hexagonal cross-section and one opposed pair of six side faces is the (001) crystal plane.

2. Experimental

The single crystals of α-Sm_2S_3 and α-Dy_2S_3 were grown by a chemical transport reaction method with iodine for carrier gas [10]. Identification of the powder sample and determination of the crystal orientation were performed by X-ray (Cu K_α radiation) diffraction measurements. The magnetic measurements were carried out using an *rf*-SQUID magnetometer with Magnetic Property Measurement System (MPMS, Quantum Design, USA). The needle-shaped single crystals having lengths of a few millimeters along the *b*-axis, distances of a few sub-millimeters across hexagonal cross section in the *ac*-plane and masses of several milligrams were mounted to the sample rotator with GE 7031 varnish. The sample rotator enables rotation of a sample around a horizontal axis in a

vertical magnetic field. The electrical resistivity was measured by 2-probe DC method using Physical Properties Measurement System (PPMS, Quantum Design, USA). The very same single crystal sample that was used for magnetic measurements was used also for the electrical measurements. Also in the electrical measurements, the sample rotator was used to rotate the sample around a horizontal axis in a vertical magnetic field.

3. Results and discussion

Figure 3 shows the temperature and magnetic field dependence of the electrical resistivity ρ for α-Sm_2S_3 [(a) and (b)] and α-Dy_2S_3 [(c) and (d)] in the low temperature range below 10 K. Here, the vertical axes denoting ρ are in logarithmic scale and the horizontal axes denoting the temperature T are in linear scale. The electrical resistivity was measured under various magnetic fields. The applied magnetic field to the α-Dy_2S_3 single crystal is along to the a-axis for the case in figure 3(c) and along to the c-axis for the case in figure 3(d). As for α-Sm_2S_3, the single crystal was mounted to the stage of the sample rotator in the state of inclining from the crystal axis about 10 degrees. Therefore, the direction of the magnetic field for the case in figure 3(a) is along ***c***', which is inclined 10 degrees from the crystal axis ***c***. In the same way, the magnetic-field direction for the case in figure 3(b) is along ***a***' being inclined 10 degrees from the crystal axis ***a***. In figure 3(a) and 3(b), the $\rho(T)$ curves under no magnetic field ($\mu_0 H = 0$ T) are understandably the same. As seen in the $\rho(T)$ curve for 0 T, the value of ρ(5.7 K) is more than 500 times larger than the value of ρ(8.0 K). The value larger than 10^5 Ω cm below $T = 5.7$ K is out of the measureable range for normal PPMS, thus the experimental curve has

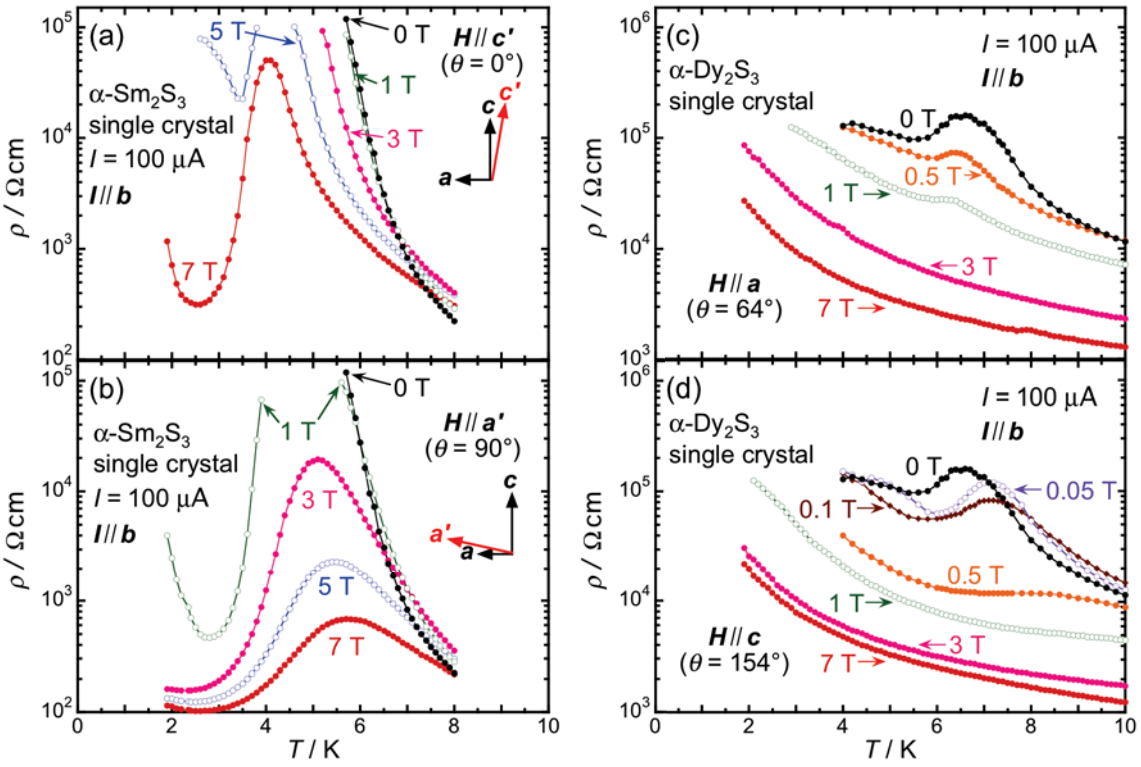

Figure 3. Temperature and magnetic field dependence of the electrical resistivity ρ for α-Sm_2S_3 [(a) and (b)] and α-Dy_2S_3 [(c) and (d)] single crystals in the low temperature range below 10 K. The vertical axes are in logarithmic scale. In the upper figures (a) and (c), the magnetic field is applied; (c) along, or (a) in the near direction of, the hard magnetization axis. While, in the lower figures (b) and (d), the magnetic field is applied; (d) along, or (b) in the near direction of, the easy magnetization axis.

ended at this point. According to the previous data taken by another measurement system, this curve forms a sharp peak with a maximum at $T = 7.0$ K [4]. Similar behavior is seen in the curves measured under the magnetic field of 1 and 3 T along ***c***' in figure 3(a). The curve for $\mu_0 H = 5$ T also resembles the curves mentioned above. However, in cooling process, the ρ gets immeasurable high values once then it returns to measurable low values. We can see whole figure of the $\rho(T)$ curve for the case of $\mu_0 H = 7$ T. Thus, the electrical resistivity shows huge enhancement in a narrow temperature range and such enhancement is suppressed by a magnetic field. If we assume all the curves in figure 3(a) have peaks, the maximum point in each peak seems to shift to lower temperature with decreasing temperature. The easy magnetization axis in the *ac*-plane of used single crystal for α-Sm_2S_3 is the *a*-axis and the hard magnetization axis is the *c*-axis, which will be shown later. Therefore, applying magnetic field in the near direction of the hard magnetization axis moves the enhanced $\rho(T)$ peak to lower temperature. Also in the case of applying magnetic field along ***a***', the enhanced $\rho(T)$ peak shrinks with increasing magnetic field as shown in figure 3(b). Peaks of three curves for $\mu_0 H = 3$, 5 and 7 T are confirmed. Moreover, it is clearly seen that the peak shifts to higher temperature with increasing magnetic field in the near direction of the easy magnetization axis. Turning now to the case for α-Dy_2S_3, although the $\rho(T)$ peak for the single crystal sample used for the present measurements is blunter than the previous result [1], the value of the ratio $\rho(6.8\text{ K})/\rho(10.0\text{ K})$ for $\mu_0 H = 0$ T is confirmed to be more than 10 in figure 3(c) and 3(d). The $\rho(T)$ peak is suppressed more rapidly by the magnetic field than the case of α-Sm_2S_3, especially it is marked for ***H***//***c*** as shown in figure 3(d). The α-Dy_2S_3 single crystal used has the easy magnetization axis along ***c*** and the hard axis along ***a*** in the *ac*-plane as shown in detail later. Therefore, also in the case of α-Dy_2S_3, the magnetic field along the hard magnetization axis; H_{hard}, shifts the $\rho(T)$ peak to lower temperature, while the magnetic field along the easy axis; H_{easy}, shifts it to higher temperature. The higher magnetic field, the larger shift we observe.

Next, let us see the magnetic-field-direction effect to the suppression of the huge ρ enhancement. We measured ρ with rotating the sample stage in fixed vertical magnetic fields at some temperatures. The rotation angle θ was changed from 0 to 360°. It is adequate to show the results as an angle dependent electrical conductivity $\sigma(\theta)$ instead of $\rho(\theta)$ because the angle dependence of ρ is not clear at the θ range in which the ρ enhancement is strongly suppressed, i.e. the ρ value in such θ range is too small relatively.

Figure 4 shows the sample-rotation-angle dependence of the electrical conductivity σ ($=1/\rho$) and the magnetization M for α-Sm_2S_3 [(a) and (b)] and α-Dy_2S_3 [(c) and (d)]. The $\sigma(\theta)$ has the same tendency regardless of the applied magnetic field strength, as well as the $M(\theta)$. Thus, we show the clearest figures for a certain magnetic field in each case. Figure 4(a), the $\sigma(\theta)$ of α-Sm_2S_3 under the magnetic field of $\mu_0 H = 7$ T, demonstrates highly anisotropic features. The $\sigma(\theta)$ shows two humps feature having 2-fold symmetry. As for the 2-fold symmetry, it is natural because the space group *Pnma* of this crystal structure has 2-fold screw axis vertical to the *ac* plane. It has two maxima at $\theta =$ 100, 280° corresponding to ***H***//***a*** and two minima at $\theta = 10$, 190° corresponding to ***H***//***c***. Although such feature is seen at the temperatures both below and above $T_{C1} = 3.8$ K, the anisotropy of $\sigma(\theta)$ below T_{C1} is larger. Below T_{C1}, the value of $\sigma(10°)$ is not specified because the $\rho(10°)$ value is too large to measure. However, at least, the $\sigma(100°)$ value is more than 200 times larger than the $\sigma(10°)$ value at $T = 3.0$ K. Let us now reorganize as follows. The $\rho(T)$ shows a huge enhancement and restoration just above T_{C1} and such enhancement is suppressed largely by a magnetic field as reported previously [4]. This suppression effect is highly anisotropic, and the suppression for the case of ***H***//***a*** is the strongest. Turning now to the $M(\theta)$ result for α-Sm_2S_3 as shown for the case of $\mu_0 H = 5$ T in figure 4(b). We displace the $M(\theta)$ figure to the left side in order to arrange the magnetic field directions between the $M(\theta)$ and $\sigma(\theta)$. The $M(\theta)$ shows similar angle dependence to that of the $\sigma(\theta)$. In this temperature range, the easy magnetization axis in the *ac*-plane for this single crystal sample is

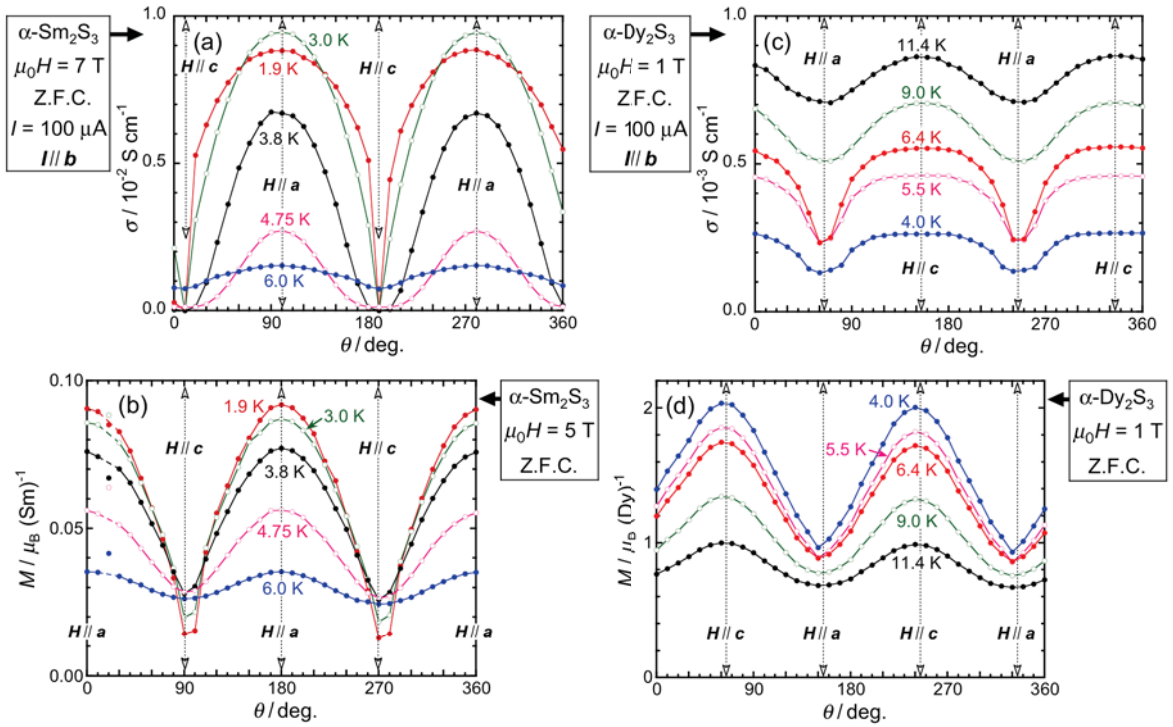

Figure 4. Sample-rotation-angle dependence of the electrical conductivity σ and the magnetization M for α-Sm_2S_3 [(a) and (b)] and α-Dy_2S_3 [(c) and (d)] single crystals at some temperatures around successive transition temperatures. The upper and lower figures are shifted relatively in order to arrange the magnetic field directions. The magnetic field directions are also shown in the figures.

the *a*-axis. Therefore, the WFM ordering of Sm moments affects the suppression of the electrical resistivity enhancement strongly. In other words, disordering state of Sm moments just before ordering is significantly related to the huge enhancement of the electrical resistivity.

Let us see the results for α-Dy_2S_3. Since the wide surface parallel to the crystal plane (101) was agglutinated to each sample stage of the sample rotators, the angles of $64°+n\cdot90°$ (n is an integer) in figure 4(c) and 4(d) correspond to the situation of the magnetic field parallel to the crystal axes. Figure 4(c) is the $\sigma(\theta)$ under $\mu_0H = 1$ T for α-Dy_2S_3. Two humps feature is similar to that of α-Sm_2S_3 qualitatively although the anisotropy is relatively small. Two maxima at θ = 154, 334° and two minima at θ = 64, 244° are observed. The former angles correspond to $\boldsymbol{H}//\boldsymbol{c}$ and the latter correspond to $\boldsymbol{H}//\boldsymbol{a}$. Common features are seen at the temperatures below T_{N1} = 11.4 K. However, the anisotropy of $\sigma(\theta)$ below T_{N2} = 6.4 K is relatively larger. The anisotropy for $T = T_{N2}$ is the largest among the measurements as $\rho(154°)/\rho(64°)$ = 2.3. The suppression of the ρ enhancement is the strongest when the magnetic field is applied along $\boldsymbol{c}$. The θ range, in which the strong suppression is observed, gets wider around 134° (and 314°) when the temperature goes below T_{N2}. Such behavior is confirmed also in the $\sigma(\theta)$ curve for $T = T_{C2}$ = 1.9 K of α-Sm_2S_3 in figure 4(a). The $\boldsymbol{c}$ for α-Dy_2S_3 single crystal used in the present measurement is the easy magnetization axis as shown in figure 4(d). Hence, the AFM ordering of Dy moments affects the suppression of the electrical resistivity enhancement strongly also in the case of α-Dy_2S_3.

4. Summary

We have investigated the suppression effect of the anomalous electrical resistivity enhancement in the α-Sm_2S_3 and α-Dy_2S_3 single crystals by applying magnetic field. The enhancement of electrical resistivity is suppressed by magnetic fields regardless of their directions; however, the strength of the

suppression significantly depends on the magnetic field direction in the *ac*-plane. It has been found that the magnetic field H_{easy} affects the $\rho(T)$ peak to move toward higher temperature, while H_{hard} moves the $\rho(T)$ peak toward lower temperature. We have examined the sample-rotation-angle dependent $\sigma(\theta)$ and $M(\theta)$ in fixed vertical magnetic fields in detail, and found highly anisotropic behavior. It has been clarified the enhanced ρ is strongly suppressed by the magnetic field H_{easy}. We have concluded that the magnetic ordering, WFM ordering in α-Sm_2S_3 and AFM ordering in α-Dy_2S_3, of *R* moments suppresses the enhancement of ρ. In other words, disordering state of *R* moments just before ordering is significantly related to the huge enhancement of the electrical resistivity.

Acknowledgments
We thank Mr. S Nakano and Mr. T Otomo for their helpful assistance in measurements and Dr. Y Shibayama for useful discussions.

References
[1] Ebisu S, Narumi M and Nagata S 2006 *J. Phys. Soc. Jpn.* **75** 085002
[2] Ebisu S, Narumi M, Gorai M and Nagata S 2007 *J. Magn. Magn. Mater.* **310** 1741-3
[3] Ebisu S, Koyama K, Omote H and Nagata S 2009 *J. Phys.: Conf. Ser.* **150** 042027
[4] Ebisu S, Omote H and Nagata S 2010 *J. Phys.: Conf. Ser.* **200** 092005
[5] Ebisu S, Koyama K, Horikoshi T, Kokita M and Nagata S 2012 *J. Phys.: Conf. Ser.* **400** 032010
[6] Ebisu S, Ushiki Y and Takahashi S 2013 *J. Korean Phys. Soc.* **63** 571-4
[7] Prewitt C T and Sleight A W 1968 *Inorganic Chemistry* **7** 1090-3
[8] Picon M, Domange L, Flahaut J, Guittard M and Patrie M 1960 *Bull. Soc. Chim. France* **2** 221-8
[9] Sleight A W and Prewitt C T, 1968 *Inorg. Chem.* **7** 2282-8
[10] Ebisu S, Iijima Y, Iwasa T and Nagata S 2004 *J. Phys. Chem. Solids* **65** 1113-20
[11] Kikkawa A, Katsumata K, Ebisu S and Nagata S 2004 *J. Phys. Soc. Jpn.* **73** 2955-8
[12] Matsuda M, Kikkawa A, Katsumata K, Ebisu S and Nagata S 2005 *J. Phys. Soc. Jpn.* **74** 1412-5
[13] Katsumata K, Kikkawa A, Tanaka Y, Shimomura S, Ebisu S and Nagata S 2005 *J. Phys. Soc. Jpn.* **74** 1598-601
[14] Ebisu S, Gorai M, Maekawa K and Nagata S 2006 *AIP Conf. Proc.* **850** 1237-8
[15] Matsuda M, Kakurai K, Ebisu S and Nagata S 2006 *J. Phys. Soc. Jpn.* **75** 074710
[16] Ebisu S, Nagata T, Fuji K and Shibayama Y 2014 *J. Phys.: Conf. Ser.* **568** 042003